RSC Advances

ROYAL SOCIETY OF CHEMISTRY

www.rsc.org/advances

Table of Contents

Anthracene-based ferrocenylselenoethers: syntheses, crystal structures, Cu(I) complexes and sensoring property

Yu-Qing Liu, Wei Ji, Hai-Yan Zhou, Yu Li, Su Jing, Dun-Ru Zhu, Jian Zhang

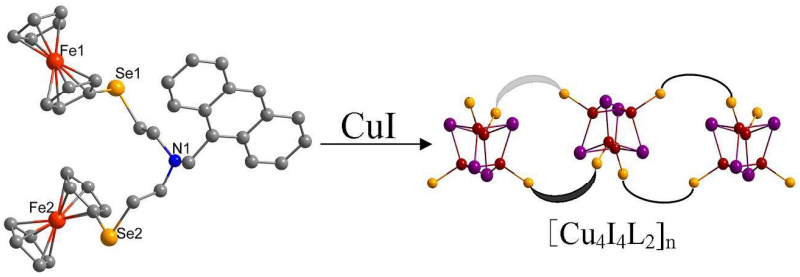

Three novel ferrocenylselenoethers containing anthracene unit and four their Cu(I) halide complexes were synthesized and structurally characterized.

Anthracene-based ferrocenylselenoethers: syntheses, crystal structures, Cu(I) complexes and sensoring property †

Yu-Qing Liu[a], Wei Ji[a,b], Hai-Yan Zhou[a], Yu Li[a], Su Jing*[,a], Dun-Ru Zhu*[,b], Jian Zhang[c]

Abstract: Three novel anthracene-based ferrocenylselenoethers, 1,5-diselena-3-(anthracen-9′-ylmethyl)-[5]ferrocenophane (**L3**), 1,3-bis(ferrocenylseleno)-2-(anthracen-9′-ylmethyl)propane (**L4**) and N,N-bis[2-(ferrocenylselena)ethyl]-N-(anthracen-9′-ylmethyl)amine (**L5**) and their Cu(I) complexes, $[Cu_2Br_2(\mathbf{L2})_2]$ (**L2** = 1,1'-bis[2-(anthracen-9′-yloxy)-ethylseleno]ferrocene) (**1**), $[Cu_2I_2(\mathbf{L2})_2]$ (**2**), $[Cu_2I_2(\mathbf{L3})_2]\cdot 1.25CH_2Cl_2$ (**3**) and $[Cu_4I_4(\mathbf{L5})_2]\cdot CH_2Cl_2$ (**4**), have been prepared and structural characterized. The X-ray crystallography analysis reveals that the complexes **1-3** possess a rhomboidal Cu_2X_2 core which is sandwiched by two **L** ligands through two Se atoms to form a dimer, while **4** owns a distorted cubane-like Cu_4I_4 core which is double-bridging linked by two **L5** ligands via two Se atoms to produce an 1D loop chain. Each Cu(I) ion in **1-4** displays a distorted tetrahedrally geometry. The unique structural feature in **L3**-**L5** is the coexistence of a redox moiety (ferrocenyl) and a fluorescent chromogenic group (anthracenyl). In the cation sensing study, **L3** and **L4** present multiresponsive signals for Cu^{2+} and Hg^{2+}, **L5** for Cu^{2+}, Zn^{2+} and Hg^{2+}. The selectivity can be tuned by incorporating additional donor atom N, and/or oxidation of the ferrocene unit.

Keywords: synthesis, crystal structure, ferrocenylselenoether, anthracene, Cu(I) complex, multichannel sensor

[a]*College of Sciences, Nanjing Tech University, Nanjing 211816, P.R. China. E-mail: sjing@njtech.edu.cn.*

[b]*College of Chemistry and Chemical Engineering, Nanjing Tech University, Nanjing 210009, P.R. China. E-mail: zhudr@njtech.edu.cn.*

[c]*Laboratory of Translational Medicine, Jiangsu Province Academy of Traditional Chinese Medicine, Nanjing 210028, P.R. China.*

[†]*CCDC numbers 1023396–1023398; 992605-992606; 1034752-1034753. For crystallographic data in CIF or other electronic format see DOI:*

Introduction

The development of efficient chemosensors for transition-metal ions with biological and environmental interest is an area of intense activity in order to address practical needs.[1,2] For example, the chemosensors for Cu^{2+} and Hg^{2+} have received considerable attention because of these ions' bioaccumulation and toxicity.[3-4] Zn^{2+} ion is the second most abundant transition metal ion in the human body, which participates in key cellular processes such as DNA repair and apoptosis.[5] Multisignaling chemosensors, built by combining chromogenic units, redox-active groups, and/or fluorescent signaling subunits, are particularly attractive in this field due to their high selectivity.[6,7] As a redox-active unit, ferrocene has been found to be one of the most favored building blocks in the construction of sensing platforms due to the availability, stability and tailorability. Although the ferrocene unit often behaves as an emission quencher due to the involvement of energy and/or electron transfer[8], it is well-known that fluorescence enhancement induced by complexation or oxidation of ferrocene unit can be achieved strategically. Fluorescence enhancement is more desirable in terms of sensitivity and selectivity. In this context, it has been observed that some multisignaling chemosensors based on N-donor ferrocenyl derivatives show a good response to Cu^{2+}, Hg^{2+} and Zn^{2+}.[9-12] However, excellent discrimination between Cu^{2+}, Hg^{2+}, Zn^{2+} and the chemically close ions still present a challenge.

Our group has embarked on the systematic study of multichannel probes based on ferrocenyl selenoethers because the soft Se atoms show a good binding property to heavy and late transition metal cations.[13-16] In the study of fluorescent sensor, anthracene was chosen as the light emitting fragment in view of its strong emission and chemical stability. Several anthracene-based ligands show selective detection of

Hg^{2+}, Cu^{2+}, Zn^{2+} through fluorescent signal.[17-21] A tetra-aza macrocycle containing a ferrocene unit and a anthracene group shows similar electrochemical responses to Cu^{2+}, Zn^{2+} and Cd^{2+}, but only gives an emission response to Cu^{2+}.[22] Two anthracene-based selenium derivatives[23] have been reported to display highly selective chelation enhanced fluorescence (CHEF) effects only with Hg^{2+} among the metal ions examined in an acetonitrile/chloroform mixture (4:1, v/v). Our previous result revealed that two Se/O mixed-donor receptors (**L1**-**L2**) containing ferrocenyl and anthracenyl moieties can display fluorescence intensity enhancement only with Cu^{2+} among the metal ions examined.[24] Inspired by such precedents, we designed three new analogous receptors with Se donor **L3**-**L4** and Se/N mixed-donor **L5**. Their multichannel sensoring properties are reported.

It is also noteworthy that di- or polynuclear neutral $(CuX)_n$ (X = halide) complexes can be used as secondary building units (SBUs) to form various complexes with interesting structures and luminescent properties.[25-27] As compared to the systematic study of $(CuX)_n$ complexes with thioethers,[28] the counterparts with the selenoethers remain less explored. Up to now, $[Cu_2X_2(\mu\text{-}SeMe_2)]_n$ (X = Cl, I) and $[Cu_4I_4(\mu\text{-}\eta^2\text{-}Me_6[12]aneSe_3)_2]$ are the only three examples reported for the $(CuX)_n$ complexes with selenoether.[29-30] Based on these considerations, we reported here the syntheses of three new receptors with Se donor (**L3**-**L5**) and their $(CuX)_n$ complexes, $[Cu_2Br_2(\mathbf{L2})_2]$ (**1**), $[Cu_2I_2(\mathbf{L2})_2]$ (**2**), $[Cu_2I_2(\mathbf{L3})_2]\cdot 1.25CH_2Cl_2$ (**3**) and $[Cu_4I_4(\mathbf{L5})_2]\cdot CH_2Cl_2$ (**4**). Their single-crystal structures and spectral properties are systematically investigated.

Experimental

Materials and physical measurements

All of the materials for synthesis were purchased from commercial suppliers and used without further purification. All of the solvents used were of analytical reagent grade. The set of metal cations used were added as perchlorate salts dissolved in acetonitrile at the concentrations described below for each of the techniques used (*WARNING: perchlorate salts are hazardous because of the possibility of explosion; only small*

amounts of this material should be handled and with great caution). NMR spectra were recorded on a Bruker DRX spectrometer operating at 300 MHz. Mass spectra were recorded using electron impact (EI) or positive ion electrospray (ES): assignments are based on isotopomers containing ^{1}H, ^{12}C, ^{14}N, ^{16}O, ^{56}Fe and ^{80}Se; expected isotope distribution patterns were observed. High-resolution MALDI mass spectra were registered on a Bruker ULTRAFLEX II TOF/TOF instrument with DCTB as the matrix. UV-visible spectra were recorded on a Perkin-Elmer 35 spectrometer. The liquid fluorescence measurements were performed at room temperature on a Perkin-Elmer LS 50B fluorescence spectrophotometer, with data collected from 200 to 1000 nm with excitation at 360 nm. Both excitation and emission slit widths were 10 nm. The solid-state emission/excitation spectra were recorded on Edinburgh instruments fluorescence spectrometer F900 at room temperature. Electrochemical measurements were performed at room temperature in a dry CH_3CN/CH_2Cl_2 (1:1, v/v) solution containing 0.1 M $[NBu_4][PF_6]$ electrolyte using an CHI 660D potentiostat system. The sweep rate for cyclic voltammetry was 100 mV s^{-1}. A three electrode arrangement was used with a Pt working electrode, a Pt wire counter electrode, and a Ag/Ag^+ (0.01 M $AgNO_3$ in CH_3CN/CH_2Cl_2, referenced against ferrocene/ferrocenium) reference electrode.

Synthesis and characterization

1-(Ferrocenylseleno)-2-(anthracen-9′-yloxy)ethane **(L1)** and 1,1'-bis[2-(anthracen-9′-yloxy)-ethylseleno]ferrocene **(L2)** were synthesized following the procedure reported in the ref. 24.

1,5-Diselena-3-(anthracen-9′-ylmethyl)-[5]ferrocenophane (**L3**). 1,2,3-Triselena[3] ferrocenophane, $fcSe_3$ (0.220 g, 0.5 mmol) (fc = $[Fe(\eta^5\text{-}C_5H_4)_2]$) was dissolved in EtOH (120 mL); $NaBH_4$ (0.19 g, 5 mmol) was then added. After stirring for 2 h, the mixture became homogeneous. A THF solution of 9-(3′-bromo-2′-bromomethylpropyl)anthracene (4 mL, 0.196 g, 0.5 mmol) was added, and the mixture left to stir for 6 h at room temperature. The solvent was removed by evaporation under reduced pressure. The residue was treated with water (50 mL) and then extracted with CH_2Cl_2 (3 × 50 mL). The extract was dried over $MgSO_4$, evaporated to dryness, then subjected to column chromatography on SiO_2. The target

product, an orange solid (0.050 g, 34.4%), was obtained by elution with hexane/dichloromethane (10:1). m.p. 179-180 °C. ^{1}H NMR δ (300 MHz, $CDCl_3$): 8.39 (s, 1H, $C_{14}H_9$, H_{10}), 8.30 (d, J = 8.4Hz, 2H, $C_{14}H_9$, H_{1+8}), 8.03 (d, J = 8.5 Hz, 2H, $C_{14}H_9$, H_{4+5}), 7.60-7.46 (m, 4H ,$C_{14}H_9$), 4.43-4.19 (m, 8H, C_5H_4), 3.75 (d, J = 7.3 Hz, 2H, $ArCH_2C$), 3.50-3.35 (m, 4H, CCH_2Se), 2.74-2.60 (m, 1H, C_3CH). MALDI-TOF-MS: *m/z* calculated: 574.24, $[M + 1]^+$; found: 575.51.

1,3-Bis(ferrocenylseleno)-2-(anthracen-9′-ylmethyl)propane (**L4**). Diferrocenyl diselenide, Fc_2Se_2 (0.264 g, 0.5 mmol) (Fc = $[Fe(\eta^5\text{-}C_5H_5)(\eta^5\text{-}C_5H_4)]$) was dissolved in EtOH (120 mL); $NaBH_4$ (0.189 g, 5 mmol) was then added. After stirring for 2 h, the mixture became homogeneous. A THF solution of 9-(3′-bromo-2′-bromomethylpropyl)anthracene (4 mL, 0.196 g, 0.5 mmol) was added, and the mixture left to stir for 5 h at room temperature. The solvent was removed by evaporation under reduced pressure. The residue was treated with water (50 mL) and then extracted with CH_2Cl_2 (3 × 50 mL). The extract was dried over $MgSO_4$, evaporated to dryness, then subjected to column chromatography on SiO_2. The target product, an orange solid (0.063 g, 32%), was obtained by elution with hexane/dichloromethane (10:1). m.p. 174-175 °C. ^{1}H NMR (300 MHz, $CDCl_3$) δ: 8.32 (s, 1H, $C_{14}H_9$, H_{10}), 8.27 (d, J = 8.6 Hz, 2H, $C_{14}H_9$, H_{1+8}), 7.98 (d, J = 8.3 Hz, 2H, $C_{14}H_9$, H_{4+5},), 7.51-7.42 (m, 4H, $C_{14}H_9$), 4.00-4.25 (m, 18H, C_5H_4 & C_5H_5), 3.73 (d, J = 7.4 Hz, 2H, $ArCH_2C$), 2.89-2.84 (m, 2H, CCH_2Se), 2.76-2.70 (m, 2H, CCH_2Se), 2.42-2.36 (m, 1H ,C_3CH). MALDI-TOF-MS: *m/z* calculated: 760.27, $[M + 1]^+$; found: 761.19.

N,N-Bis[2-(ferrocenylselena)ethyl]-N-(anthracen-9′-ylmethyl)amine (**L5**). Fc_2Se_2 (0.6864 g, 1.3 mmol) (Fc = $[Fe(\eta^5\text{-}C_5H_5)(\eta^5\text{-}C_5H_4)]$) was dissolved in EtOH (120 mL); $NaBH_4$ (0.5394 g, 13 mmol) was then added. After stirring for 2 h, the mixture became homogeneous. A THF solution of N,N-dibromoethyl-N-(9-anthracenylmethyl)amine (0.60 g, 1.43 mmol) was added, and the mixture left to stir for 18 h at room temperature. The solvent was removed by evaporation under reduced pressure. The residue was treated with water (50 mL) and then extracted with CH_2Cl_2 (3 × 50 mL). The extract was dried over $MgSO_4$,

evaporated to dryness, then subjected to column chromatography on SiO_2. The target product, an orange solid (0.43 g, 42%), was obtained by elution with hexane/dichloromethane (1:1). m.p. 110-111 °C. ^{1}H NMR (300 MHz, $CDCl_3$) δ: 8.45 (s, 1H, $C_{14}H_9$, H_{10}), 8.40 (d, J = 10.1 Hz, 2H, $C_{14}H_9$, H_{1+8}), 7.98 (d, J = 7.7 Hz, 2H, $C_{14}H_9$, H_{4+5}), 7.49-7.44 (m, 4H, $C_{14}H_9$), 4.50 (s, 2H, $ArCH_2N$), 4.09 (s, 10H ,C_5H_5), 4.03 (dd, J = 4.0, 1.5 Hz, 8H, C_5H_4), 2.82-2.77 (m, 4H, NCH_2C), 2.62-2.57 (m, 4H, CCH_2Se). ESI-MS: *m/z* calculated: 790.32, $[M + 1]^+$; found: 792.00.

$[Cu_2Br_2(\mathbf{L2})_2]$ (**1**). **L2** (0.039 g, 0.05 mmol) was dissolved in dichloromethane (2 mL), CuBr (0.0072 g, 0.05 mmol) was dissolved in acetonitrile (2 mL), **1** was grown by slow diffusion of a dichloromethane solution of **L2** into a acetonitrile solution of CuBr at room temperature. Orange lamellar crystals of **1** were obtained in two weeks (0.018 g, 19.4%). m.p. 185-186°C. Elemental analysis calcd (%) for **1**. $C_{84}H_{68}Br_2Cu_2Fe_2O_4Se_4$: C, 54.36; H, 3.69. Found: C, 54.12; H, 3.31.

$[Cu_2I_2(\mathbf{L2})_2]$ (**2**). **L2** (0.039 g, 0.05 mmol) was dissolved in dichloromethane (2 mL), CuI (0.0095 g, 0.05 mmol) was dissolved in acetonitrile (2 mL), **2** was grown by slow diffusion of a dichloromethane solution of **L2** into a acetonitrile solution of CuI at room temperature. Orange lamellar crystals of **2** were obtained in in two weeks (0.023 g, 24%). m.p. 182-183°C. Elemental analysis calcd (%) for **2**. $C_{84}H_{68}Cu_2Fe_2I_2O_4Se_4$: C, 51.74; H, 3.52. Found: C, 51.52; H, 3.18.

$[Cu_2I_2(\mathbf{L3})_2]\cdot 1.25CH_2Cl_2$ (**3**). **L3** (0.028 g, 0.05 mmol) was dissolved in dichloromethane (2 mL), CuI (0.0095 g, 0.05mmol) was dissolved in acetonitrile (2 mL), **3** was grown by slow diffusion of a dichloromethane solution of **L3** into a acetonitrile solution of CuI at room temperature. Orange needles crystals of **3** were obtained in two weeks (0.012g, 14%). m.p. 254-255°C. Elemental analysis calcd (%) for **3**. $C_{57.25}H_{48.50}Cl_{2.50}Cu_2Fe_2I_2Se_4$: C, 42.09; H, 2.99. Found: C, 41.81; H, 2.77.

$[Cu_4I_4(\mathbf{L5})_2]\cdot CH_2Cl_2$ (**4**), **L5** (0.0395 g, 0.05 mmol) was dissolved in dichloromethane (2 mL), CuI (0.0095 g, 0.05 mmol) was dissolved in acetonitrile (2 mL), **4** was grown by slow diffusion of a dichloromethane solution of **L5** into a acetonitrile solution of CuI at room temperature. Orange needles crystals of **4** were obtained in two weeks (0.029 g, 6%). m.p. 150-151°C. Elemental analysis calcd (%)

for **4**. $C_{316}H_{304}Cl_8Cu_{16}Fe_{16}I_{16}N_8Se_{16}$: C, 39.12; H, 3.16; N,1.16. Found: C, 38.87; H, 2.97; N,1.01.

X-ray data collection and structural determination

All of the single crystal X-ray diffraction data were obtained on a Bruker SMART APEX II CCD diffractometer using graphite-monochromatized Mo K_α radiation (λ = 0.71073 Å) at room temperature. A hemisphere of data was collected using a narrow-frame method with scan widths of 0.30° in ω and an exposure time of 10 s/frame. Data were integrated using the Siemens SAINT program, with intensities corrected for Lorentz factor, polarization, air absorption, and absorption due to variation in the path length through the detector faceplate. Multiscan absorption corrections were applied. Structures were solved by direct methods and refined on F^2 by full-matrix least-squares using SHELXTL. All non-hydrogen atoms were located from the Fourier maps and refined anisotropically. All H atoms were refined isotropically with the isotropic vibration parameters related to the non-H atom to which they are bonded. The structure of **3** was refined using the solvent masking routine, SQUEEZE (Platon), as it was difficult to identify and model the solvent present in the lattice. The crystal undergoes decomposition/solvent loss during data collection adding to the problem.

UV-vis and fluorescence detection of metal ions

Stock solutions (0.15 M) of the perchlorate salts of Li^+, Na^+, K^+, Ca^{2+}, Mg^{2+}, Ni^{2+}, Cd^{2+}, Zn^{2+}, Pb^{2+}, Hg^{2+} and Cu^{2+} in acetonitrile were prepared. Solutions of **L3-L5** (100 μM) were also prepared in CH_2Cl_2. 80 μL of stock solutions (0.15 M) of the metal perchlorate salts were transferred to 3 mL of a solution of **L3-L5** (100 μM). After mixing them for a few seconds, the UV-vis and fluorescence properties were tested.

UV-vis titrations of L5 with Zn^{2+} and Cu^{2+}

L5 was dissolved in CH_2Cl_2 to make a 100 μM solution. Stock solutions (0.15 M) of the perchlorate salts of Zn^{2+} and Cu^{2+} in acetonitrile were prepared. 0-24 μL of $Zn(ClO_4)_2$ (0.15 M) was transferred to separate receptor solutions (100 μM, 3 mL). 0-100 μL of $Cu(ClO_4)_2$ (0.15 M) was transferred to separate receptor solutions (100

μM, 3 mL). After mixing them for a few seconds, UV-vis spectra were obtained at room temperature.

Results and discussion

Synthesis

The ligands **L3-L5** were synthesized in stepwise manner, as shown in Scheme 1. The crystals of **L3-L5** were obtained by slow evaporation of a solution in a mixture of *n*-hexane and dichloromethane (3:1, v/v). Diffusion of a dichloromethane solution of **L2**, **L3** or **L5**, respectively, into a MeCN solution of CuX (X = Br or I) afforded four Cu(I) complexes, $[Cu_2X_2(\mathbf{L2})_2]$ (**1**, X = Br; **2**, X = I), $[Cu_2I_2(\mathbf{L3})_2]\cdot 1.25CH_2Cl_2$ (**3**) and $[Cu_4I_4(\mathbf{L5})_2]\cdot CH_2Cl_2$ (**4**). **L3-L5** and **1-4** were further characterized by X-ray diffraction analysis. All data are in agreement with the proposed structures.

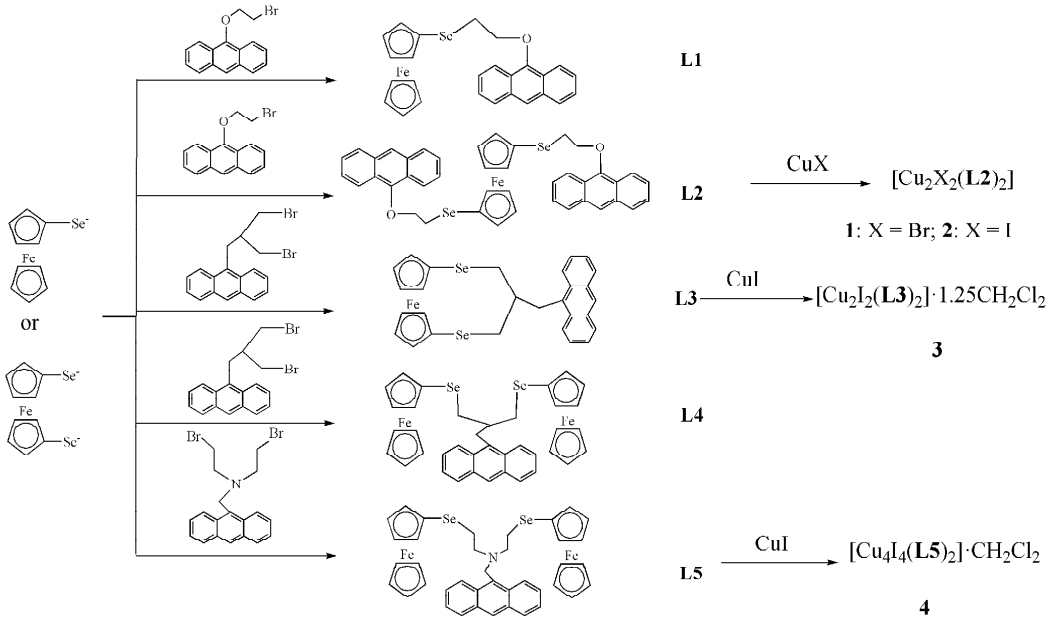

Scheme 1. Synthetic routes for **L1-L5** and **1-4**.

Crystal structures

Major structural parameters are summarized in Table 1 for **L3-L5** and Table 2 for **1-4**. Selected bond lengths and angles are given in Tables S1 and S2 (ESI). ORTEP plots of **L3-L5** and **1-4** are shown in Figures 1-3.

(Tables 1 and 2 here)

The X-ray structure analysis reveals that both **1** and **2** are a dimer composed of two ligands **L2** and two CuX molecules (Fig. 2). The two μ_2-halide ions link two Cu(I) ions to form a rhomboid plane Cu_2X_2. Then two ligands **L2** coordinate to the Cu(I) ions *via* the two selenium atoms with the oxygen atoms remaining uncoordinated. It was found that the free ligand **L2** exhibits a *trans* configuration, and the two anthracene units are parallel to each other owing to the centre of symmetry.[24] After complexation, the two anthracene units of **L2** are no longer parallel and have a dihedral angle of 38.72° in **1** and 37.30° in **2**. The ferrocene unit adopts the staggered conformation with a Cp(centroid)-Fe-Cp(centroid) torsional angle of 2.08° in **1** and 2.58° in **2**. Each Cu(I) center is a distorted tetrahedral geometry with a Se1-Cu-Se2 angle of 114.55(2)° in **1** and 112.40(2)° in **2**. The plane defined by the Cu, Se1, Se2, and the plane Cu_2X_2 forms an angle of 86.08° in **1** and 87.20° in **2**. As listed in Table S1, the Cu-X distances elongate with an increase in the covalent radius of X^-. The Cu···Cu distances in **1** and **2** are similar (2.793 and 2.782 Å, respectively), which is slightly shorter than the sum of van der Waals radii of two Cu(I) atoms (2.80 Å), indicating a weak interaction between them. The X···X separation (X = Br, 4.080 Å; X = I, 4.427 Å) is close to the usual van der Waals contact distance.

The asymmetric unit of **3** has two **L3** ligands and 1.25 CH_2Cl_2 molecules (Fig. 2). There are two crystallographically different Cu(I) ions, two μ_2-I^- ions. The two μ_2-I^- ions connect two Cu(I) ions to form a rhomboidal Cu_2I_2 core which then is sandwiched by two **L3** ligands through two Se atoms. The atoms Cu1, Se1, C11, C12, C13 and Se2 form a chair conformation, so do for the atoms Cu2, Se3, C41, C42, C43 and Se4. Both Cu1 and Cu2 centre display a considerably distorted tetrahedron with a Se1-Cu1-Se2 angle of 99.72(6)° and a Se3-Cu2-Se4 angle of 99.36(6)°. The ferrocene unit adopts the synperiplanar conformation with Cp(centroid)-Fe-Cp(centroid) torsional angles of 4.962° and 4.307°, similar to that in the free **L3** ligand (5.034°) as shown in Fig. 1. The Cu···Cu distance is 2.612(2) Å, which is quite shorter than those found in **1** and **2**, indicating a strong interaction between two Cu(I) ions. In addition, the Cu(I)-Se distances (2.430-2.454 Å) in **1-3** are similar to those observed in an

analogous complex $[Cu_2(\mu\text{-}I)_2(\mu\text{-}SeMe_2)_2]_n$.[29]

The asymmetric unit of **4** contains four crystallographically independent Cu(I) ions, four μ_3-I^- ions, two **L5** ligands and one CH_2Cl_2 guest molecule (Fig. 3a). Four Cu(I) ions are linked together through four μ_3-I^- ions to form a distorted cubane-like neutral SBU (Cu_4I_4). Each Cu(I) ion in the SBU shows a distorted tetrahedron consisting of three μ_3-I^- ions and one Se donor of **L5**. Each SBU is further interconnected to two adjacent ones by two bridge-linking **L5** ligands *via* two Se atoms to generate one extended 1D loop chain (Fig. 3b and 3c). In other words, two **L5** ligands connect two SBUs to produce a 20-member macrocycle. The Cu(I)-Se bond distances range from 2.415(2) to 2.436(2) Å, which are shorter than those observed in **1-3** and an analogous cluster $[Cu_4I_4(\mu\text{-}\eta^2\text{-}Me_6[12]aneSe_3)_2]$.[30] The Cu···Cu distances are 2.752(2)-2.893(2) Å, similar to those in the reported Cu_4I_4 cluster.[31-33]

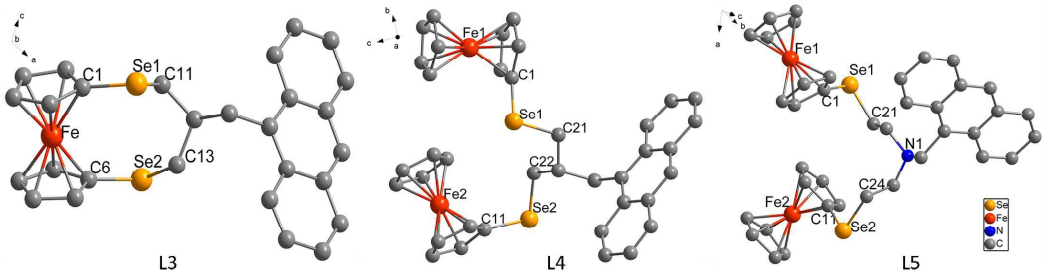

Fig. 1 View of the structures of **L3-L5** with the atomic numbering scheme. Hydrogen atoms are omitted for clarity.

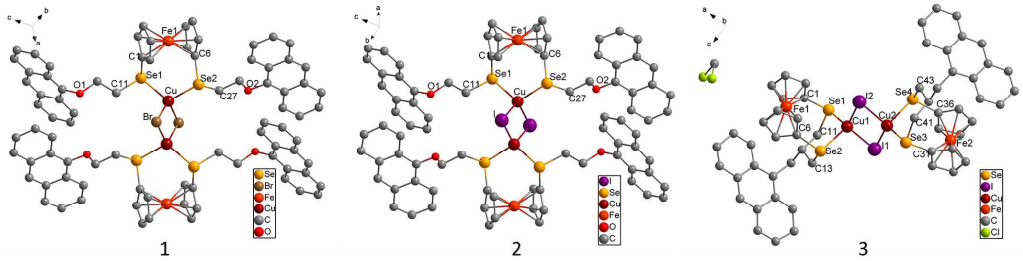

Fig. 2 View of the structures of **1-3** with the atomic numbering scheme. Hydrogen atoms are omitted for clarity.

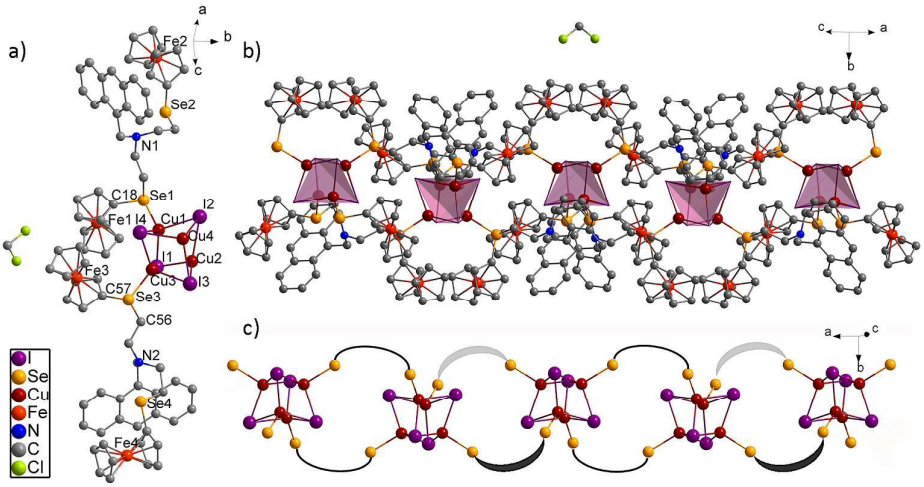

Fig. 3 (a) The asymmetric unit of **4**. (b) The 1D loop chain structure of **4**. (c) A simplified view of 1D loop chain structure of **4**. Hydrogen atoms are omitted for clarity.

Cation sensing studies

It has been found that, upon addition of transition metal ions, the "switch-on" fluorescence property of ferrocene derivatives may due to complexation[34-37] or oxidation of ferrocene unit.[38] The two mechanisms have also been demonstrated in our previous studies.[15,24] Preliminary study showed that both **L1** and **L2** displayed fluorescence intensity enhancement only with Cu^{2+} among the metal ions examined.[24] Electrochemistry and UV-vis spectra studies showed that Cu^{2+} induces the oxidation of the ferrocene unit and then forms a stable [**L1**·**L1**$^{+}$·Cu^{+}] or [**L2**$^{+}$·Cu^{+}] complex. Addition of Hg^{2+} induces fluorescence quenching and complexation with the neutral ligand.

The sensing properties of **L3**-**L5** toward some metal ions (Li^{+}, Na^{+}, K^{+}, Ca^{2+}, Mg^{2+}, Ni^{2+}, Cd^{2+}, Zn^{2+}, Pb^{2+}, Hg^{2+} and Cu^{2+}) were investigated by spectroscopic measurements and electrochemistry in CH_2Cl_2 at room temperature.

Similar to the results of **L1** and **L2**, the fluorescence spectra of free **L3**-**L5** exhibit a weak monomeric emission of anthracene at 420 nm upon excited at 365 nm. This result can be ascribed to intramolecular singlet state quenching of the fluorophore by the ferrocenyl redox center.[8] In addition, it is also possible that there is an electron

transfer process from the proximate tertiary amine nitrogen atom to the excited state of the anthracene unit in **L5**. **L3-L4** displayed fluorescence intensity quenching only with Cu^{2+} and Hg^{2+} among the tested cations (Fig. S7 and Fig. S8). Upon addition of Zn^{2+}, the emission peak of **L5** shifted from 419 to 422 nm with a simultaneous enhancement of fluorescence intensity, the maximum 5-fold fluorescence intensity enhancement was readily obtained when 1 equivalent of Zn^{2+} was introduced. The addition of 3 equivalents of Cu^{2+} caused a maximum 4-fold intensity enhancement of **L5** and slight blue shift of 4 nm (Fig. 4). Addition of Hg^{2+} induces fluorescence quenching of **L5**. **L5** does not undergo any considerable change in its emission spectrum upon addition of Li^{+}, Na^{+}, K^{+}, Ca^{2+}, Mg^{2+}, Ni^{2+}, Cd^{2+} and Pb^{2+} ions.

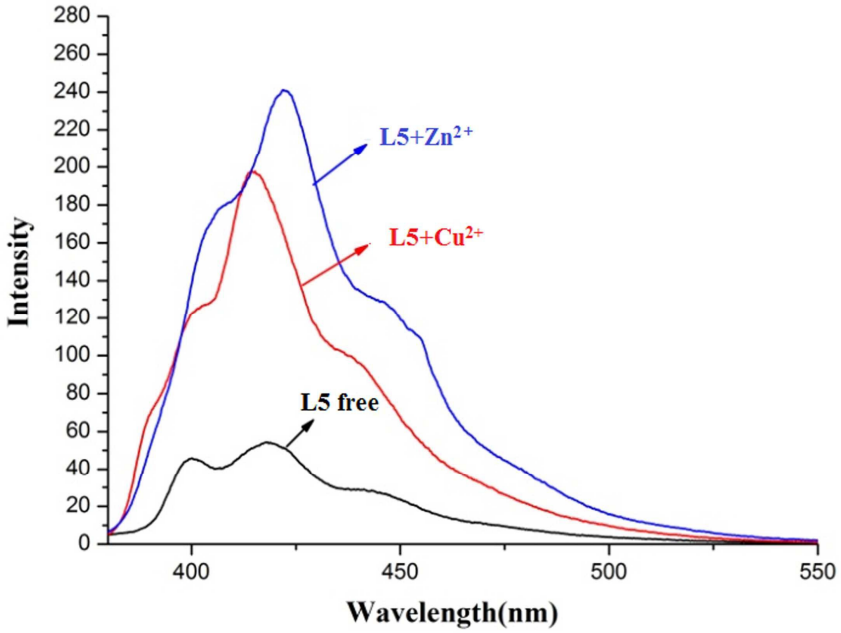

Fig. 4 Changes in the fluorescence spectra of **L5** (black, 1×10^{-4} M) in CH_2Cl_2 solution upon the addition of 1 equivalent of Zn^{2+} (blue) or 3 equivalents Cu^{2+} (red).

UV-vis spectra of **L3-L5** exhibit an absorption maximum at about 369 nm, which can be attributed to the characteristic absorption of the anthracene group.[19-20] Similar to the behaviour of **L1-L2**, addition of Cu^{2+} to solutions of **L3-L5** caused slight increase in the intensity of the high energy band and progressive appearance of two new low energy bands located at about λ = 441 and 939 nm. The changes in the

absorption spectra are accompanied by color changes from colorless to orange, which provide the potential for "naked eye" detection. The band around 441 nm can be ascribed to a MLCT transition of the Cu^{+} complex, and the one around 900 nm to the oxidized $\mathbf{L}^{+}$.[24,38-40] The addition of Zn^{2+} only induce a decrease of the absorbance of **L5** at 369 nm accompanying a small bathochromic shift, no detectable color change can be observed. Addition of Hg^{2+} to solutions of **L3-L5** caused the appearance of one new band located at about 463 nm and the color of the solution changed from colorless to orange.

Detailed titration experiments in CH_2Cl_2 solutions of **L5** with Zn^{2+} or Cu^{2+} were performed and analyzed quantitatively.[41] The saturated spectra were readily obtained when 1 equivalent of Zn^{2+} was introduced, which confirms the formation of 1:1 adduct with Zn^{2+}. The calculated association constant and detection limit of Zn^{2+} are 1.65×10^{4} M^{-1} and 6.62×10^{-6} M. For Cu^{2+}, the saturated spectra were readily obtained when 3 equivalents of Cu^{2+} was introduced, and the calculated association constant and detection limit are 1.01×10^{3} M^{-1} and 5.26×10^{-5} M.

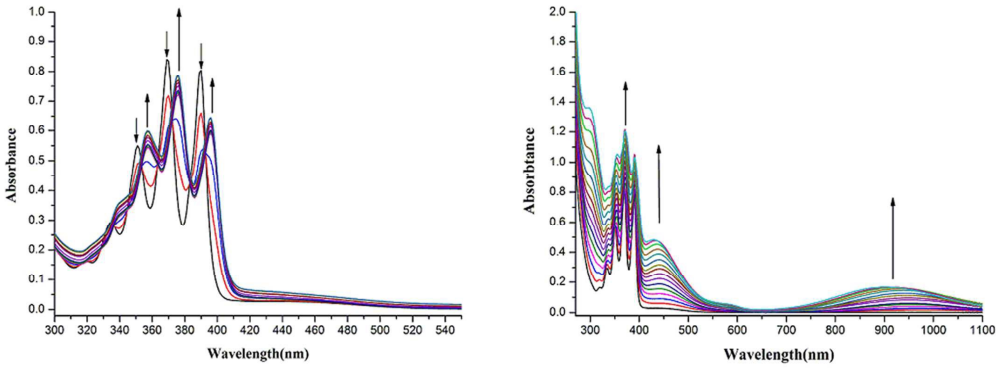

Fig. 5 UV-vis spectral changes for receptor **L5** in CH_2Cl_2 solution (1×10^{-4} M) upon the sequential addition of (a) 0 to 1.2 equivalent of $Zn(ClO_4)_2$, or (b) 0 to 5.0 equivalents of $Cu(ClO_4)_2$.

The reversibility and relative potentials of the redox processes in **L3-L5** were investigated by cyclic voltammetry (CV) in CH_3CN/CH_2Cl_2 (1:1, v/v) solutions. The voltammograms show one reversible one-electron redox couple due to the

ferrocene/ferrocenium oxidation process and one irreversible oxidation peak for the anthracene unit. In contrast to the behavior of **L1** and **L2**,[24] for **L3-L5** a less negative or more positive shift in the redox potential of the ferrocene unit is observed between the Cu^{2+} complex and the free ligand. The addition of Hg^{2+} to **L3-L5** also causes a positive shift, and Zn^{2+} has the same effect on **L5**. The significant positive shift of oxidation potential of the anthracene unit is observed upon the addition of Cu^{2+}, Zn^{2+} or Hg^{2+} to **L5**.

(Table 3 here)

It is well known that the paramagnetic Cu^{2+} has a pronounced quenching effect on fluorescent ligands, most of the earlier reports of Cu^{2+} sensors are based on quenching of fluorescence.[42-44] Literature work showed that Cu^{2+} can oxidize ferrocene unit into ferrocenium unit. Then the resonance energy transfer from the excited state of fluorophore to the ferrocenium unit cannot take place efficiently. At the same time, Cu^{2+} is reduced to non-quenching Cu^{+} because of its d^{10} electron configuration. Fluorescence enhancement is then obtained synergetically.[38] In our preliminary study, Se/O mixed-donor **L1** and **L2** displayed fluorescence intensity enhancement only with Cu^{2+} among the metal ions examined.[24] To illuminate the effect of mixed donors, the current study is performed and showed that although Cu^{2+} induces the oxidation of the ferrocene unit and then complexation in **L1-L5**, only mixed-donor sensors give fluorescence enhancement. So N or O atom is crucial to tune the energy of excited state of anthrancene and leads to the fluorescence enhancement.

The interaction between Zn^{2+} and the tertiary amine in **L5** lowers the energy of the tertiary amine and prevents electron transfer on a thermodynamic basis, resulting in fluorescence recovery.[45-48] Although Zn^{2+} and Cu^{2+} all induce fluorescence enhancement of **L5**, excellent discrimination can be obtained from UV-vis spectral changes. Fluorescence quenching is observed in the case for Hg^{2+} with **L1-L5** due to the heavy metal enhanced intersystem crossing.[49] So with the systematic study of anthracene-ferrocenylselenoethers, Se/N mixed-donor **L5** is found to show good selectivity to Cu^{2+}, Zn^{2+} and Hg^{2+} through multichannel signals.

Photoluminescence properties of 1-4

Solid-state photoluminescence studies were carried out for **1-4** at room temperature. The Cu_2X_2 dimer in **1-3** was found to be non-emissive. Although a cluster-centered excited state with mixed halide-to-metal charge transfer character is expected, the cubane-like **4** exhibits only a weak emission maximum when excited at 380 nm, presumably due to the quenching effect of the ferrocene unit.

Conclusion

We have designed and synthesized three novel anthracene-based ferrocenylselenoether ligands and four of their Cu(I) complexes. The structural analysis shows that the complexes **1-3** are a dimer, and **4** owns an 1D loop chain consisting of a 20-member macrocycle. In the cation sensing study, **L3-L5** behave as the multiresponsive chemosensors, with **L3** and **L4** for Cu^{2+} and Hg^{2+}, **L5** for Cu^{2+}, Zn^{2+} and Hg^{2+}. Cu^{2+} induces the oxidation of the ferrocene unit in **L3-L5**, but only the N mixed-donor sensor **L5** shows fluorescence enhancement. The coordination of Zn^{2+} with the N donor in **L5** leads to fluorescence enhancement. The heavy metal effect of Hg^{2+} causes fluorescence quenching of **L3-L5**. Although multichannel sensors have been developed for more than ten years, the design strategy is still a challenge. We expect that our results may provide a useful guide to design the multichannel molecular sensor.

Acknowledgements

We gratefully acknowledge financial support from the National Natural Science Foundation of China (Grant Nos. 21171092, 21171093, 21476115) and National Basic Research Program of China (973 Program) (No. 2013CB733504). The authors also thank Dr. Christopher P. Morley (Cardiff University, UK) for his valuable suggestions for this work.

References

1 U. E. Spichiger-Keller, *Chemical Sensors and Biosensors for Medical and*

Biological Applications, Wiley-VCH: Weinheim, New York, 1998.

2 J. J. R. F.-D. Silva, *The Biological Chemistry of the Elements: The Inorganic Chemistry of Life*, ed. R. J. P. Williams, Oxford University Press, New York, 2nd edn., 2001, pp. 538-549.

3 D. W. Boening, *Chemosphere,* 2000, **40**, 1335.

4 S. Horiguchi, T. Kurono and K.Teramoto, *Osaka City Med. J.,* 1983, **292**, 145.

5 P. Jiang and Z. Guo, *Coord. Chem. Rev.,* 2004, **248**, 205.

6 P. Molina, A. Tárraga and A. Caballero, *Eur. J. Inorg. Chem.,* 2008, 3401.

7 D. Jiménez, M.-M. Ramón, F. Sancenón and J. Soto, *Tetrahedron Lett.*, 2004, **45**, 1257.

8 S. Fery-Forgues and B. Delavaux-Nicot, *J. Photochem. Photobiol. A: Chem.,* 2000, **132**, 137.

9 T. Arunabha, S. Sinjinee and G. Sundargopal, *Inorg. Chem.,* 2011, **50**, 7066.

10 K. K. Chakka , *Eur. J. Inorg. Chem.,* 2013, 6019.

11 M. Alfonso, A. Tárraga and P. Molina, *Inorg. Chem.,* 2013, **52**, 7487.

12 H. Yang, Z.-G. Zhou, K.-W. Huang, M.-X. Yu, F.-Y. Li, T. Yi and C.-H. Huang, *Org. Lett.,* 2007, **9**, 4729.

13 S. Jing, C. P. Morley, C. A. Webster and M. D. Vaira, *Dalton Trans.,* 2006, 4335.

14 W. Ji, S. Jing, Z.-Y Liu, J. Shen, J. Ma, D.-R. Zhu, D.-K. Cao, L.-M. Zheng and M.-X. Yao, *Inorg. Chem.,* 2013, **52**, 5786.

15 F. Xiao, J. Shen, J. Qu, S. Jing and D.-R. Zhu, *Inorg. Chem. Commun.,* 2013, **35**, 69.

16 Y.-Z. Qin, W. Ji, F. Xiao, X. Zhang and S. Jing, *Inorg. Chem. Commun.,* 2012, **20**, 177.

17 G. D. Santis, L. Fabbrizzi, M. Licchelli, C. Mangano and D. Sacchi, *Inorg. Chem.,* 1995, **34**, 3581.

18 A. Tamayo, B. Pedras, C. Lodeiro, L. Escriche, J. Casabó, J. L. Capelo, B. Covelo, R. Kivekäs and R. Sillanpää, *Inorg. Chem.,* 2007, **46**, 7818.

19 A. Tamayo, C. Lodeiro, L. Escriche, J. Casabó, B. Covelo and P. González, *Inorg. Chem.,* 2005, **44**, 8105.

20 A. Tamayo, L. Escriche, J. Casabó, B. Covelo and C. Lodeiro, *Eur. J. Inorg. Chem.,* 2006, 2997.

21 L. Prodi, F. Bolletta, M. Montalti and N. Zaccheroni, *Coord. Chem. Rev.,* 2000, **205**, 59.

22 F. Sancenon, A. Benito, F. J. Hernández, J. M. Lloris, R. M.-Máñez, T. Pardo and J. Soto, *Eur. J. Inorg. Chem.,* 2002, 866.

23 Y. J. Lee, D. Seo, J. Y. Kwon, G. Son, M. S. Park, J. H. Sho, H. N. Lee, K. D. Lee and J. Yoon, *Tetrahedron,* 2006, **62**, 12340.

24 J. Shen, T. Liu, Y. Li, W. Ji, S. Jing, D.-R. Zhu and G.-F. Guan. *Inorg. Chem. Commun.,* 2014, **44**, 6.

25 P. C. Ford, E. Cariati and J. Bourassa, *Chem. Rev.,* 1999, **99**, 3625.

26 M. Vitale and P. C. Ford, *Coord. Chem. Rev.,* 2001, **219-221**, 3.

27 N. Armaroli, G. Accorsi, F. Cardinali and A. Listorti, *Top. Curr. Chem.,* 2007, **280**, 69.

28 P. D. Harvey and M. Knorr. *Macromol. Rapid Commun.,* 2010, **31**, 808.

29 S. Mishra, E. Jeanneau and S. Daniele, *Polyhedron,* 2010, **29**, 500.

30 R. D. Adams and K. T. McBride, *Organometallics,* 1997, **16**, 3895.

31 T. H. Kim, K. Y. Lee, Y. W. Shin, S.-T. Moon, K.-M. Park, J. S. Kim, Y. Kang , S. S. Lee and J. Kim, *Inorg. Chem. Commun.,* 2005, **8**, 27.

32 S. M. Aly, A. Pam, A. Khatyr, M. Knorr, Y. Rousselin, M. M. Kubicki, J. O. Bauer, C. Strohmann and P. D. Harvey, *J. Inorg. Organomet. Polym.,* 2014, **24**, 190.

33 C. Xie, L. Zhou, W.-X Feng, J.-K. Wang and W. Chen, *J. Mol. Struct.,* 2009, **921**, 132.

34 F. Otón, M. C. González, A. Espinosa, A. Tárraga and P. Molina, *Organometallics,* 2012, **31**, 2085.

35 Z.-P. Liu, C.-L. Zhang, Y.-L. Li, Z.-Y. Wu, F. Qian, X.-L. Yang, W.-J He, X. Gao and Z.-J. Guo, *Org. Lett.,* 2009, **11**, 795.

36 L. Xue, C. Liu and H. Jiang, *Org. Lett.,* 2009, **11**,1655.

37 L. Xue, Q. Liu and H. Jiang, *Org. Lett.,* 2009, **11**, 3454.

38 R. Martínez, I. Ratera, A. T. Tárraga, P. Molina and J. Veciana, *Chem. Commun.*, 2006, 3809.

39 F. Otón, A. Tárraga, A. Espinosa, M. D. Velasco and P. Molina, *Dalton Trans.,* 2006, **30**, 3685.

40 M. Alfonso, A. Tárraga and P. Molina, *J. Org. Chem.,* 2011, **76**, 939.

41 M. Shortreed, R. Kopelman, M. Kuhn and B. Hoyland, *Anal. Chem.*, 1996, **68**, 1414.

42 S. H. Kim, J. S. Kim, S. M. Park and S. K. Chang, *Org. Lett.*, 2006, **8**, 371.

43 J. Xie, M. Ménand, S. Maisonneuve and R. Métivier, *J. Org. Chem.*, 2007, **72**, 5980.

44 H. S. Jung, P. S. Kwon, J. W. Lee, J.I. Kim, C. S. Hong, J. W. Kim, S. H. Yan, J. Y. Lee, J. H. Lee, T. H. Joo and J. S. Kim, *J. Am. Chem. Soc.*, 2009, **131**, 2008.

45 R. A. Bissell, A. P. de Silva, H. Q. N. Gunaratne, P. L. M. Lynch, G. E. M. Maguire, C. P. McCoy and K. R. A. S. Sandanayake, *Top. Curr. Chem.*, 1993, **168**, 223.

46 A. P. de Silva, H. Q. N. Gunaratne, T. Gunnlaugsson, A. J. M. Huxley, C. P. McCoy, J. T. Rademacher and T. E. Rice, *Chem. Rev.*, 1997, **97**, 1515.

47 G. D. Santis, L. Fabbrizzi, M. Licchelli, C. Mangano and D. Sacchi, *Inorg. Chem.,* 1995, **34**, 3581.

48 F. Qian, C.-L. Zhang, Y.-M. Zhang, W.-J. He, X. Gao, P. Hu and Z.-J. Guo, *J. Am. Chem. Soc.*, 2009, **131**, 1460.

49 D. S. McClure, *J. Chem. Phys.*, 1952, **20**, 682.

Table 1. Crystallographic data for **L3-L5**.

Ligand	**L3**	**L4**	**L5**
Formula	$C_{28}H_{24}FeSe_2$	$C_{38}H_{34}Fe_2Se_2$	$C_{39}H_{38}Fe_2NSe_2$
M_r	574.24	760.27	790.32
Crystal system	Monoclinic	Orthorhombic	Triclinic
Space group	*Cc*	$P2_1/c$	*P-1*
T (K)	296(2)	293(2)	293(2)
$a/b/c$ (Å)	27.419(8)/6.081(2)/13.987(4)	5.897(6)/12.064(1)/42.577 (5)	10.728(2)/10.821(2)/16.282(2)
$\alpha/\beta/\gamma$ (°)	90/107.285(3)/90	90/90/90	76.004(2)/73.266(2)/65.170(2)
V (Å^3)	2226.7(1)	3028.9(6)	1626.9(4)
Z	4	4	2
D_{calc} (Mg·m^{-3})	1.713	1.667	1.613
μ (mm^{-1})	3.960	3.388	3.158
Reflections measured	7314	26446	11657
Independent reflections	3577	7480	5691
θ range (°)	1.56-25.00	2.22-28.31	1.32-25.00
R_{int}	0.0306	0.0323	0.0417
R_1[a]	0.0339	0.0389	0.0397
R_w[a]	0.0769	0.0842	0.1044
GOF	1.000	1.052	1.068
CCDC Deposition	1023396	1034752	992605

[a] $R = \Sigma ||F_o| - |F_c|| / \Sigma |F_o|$ and $R_w = (\Sigma \omega(|F_o| - |F_c|)^2 / \Sigma \omega F_o^2)^{1/2}$.

Table 2. Crystallographic data for **1-4**.

Complex	**1**	**2**	**3**	**4**
Formula	$C_{84}H_{68}Br_2Cu_2Fe_2O_4Se_4$	$C_{84}H_{68}Cu_2Fe_2I_2O_4Se_4$	$C_{57.25}H_{48.50}Cl_{2.50}Cu_2Fe_2I_2Se_4$	$C_{316}H_{304}Cl_8Cu_{16}Fe_{16}I_{16}N_8Se_{16}$
M_r	1855.82	1949.80	1633.51	9701.27
Crystal system	Triclinic	Triclinic	Orthorhombic	Monoclinic
Space group	*P-1*	*P-1*	$Pca2_1$	$P2_1/c$
T (K)	293(2)	293(2)	296(2)	296(2)
$a/b/c$ (Å)	8.445(2)/14.201(2)/15.545(2)	8.533(1)/14.357(2)/15.512(2)	22.737(1)/7.614(4)/32.672(2)	18.630(1)/15.465(8)/32.756(1)
$\alpha/\beta/\gamma$(°)	94.931(2)/102.002(2)/90.115(2)	85.587(2)/79.112(2)/ 89.858(2)	90/90/90	90/120.177(2)/90
V(Å^3)	1816.4(4)	1860.3(4)	5655.8(5)	8158.2(7)
Z	1	1	4	1
D_{calc} (Mg·m^{-3})	1.697	1.740	1.918	1.975
μ (mm^{-1})	4.125	3.783	5.065	5.118
Reflections measured	12972	13294	36561	16017
Independent reflections	6323	6481	6323	16017
θ range (°)	2.47-24.31	1.34-25.00	1.36-26.00	1.36-26.00
R_{int}	0.0318	0.0551	0.0422	0.1097
R_1[a]	0.0350	0.0399	0.0575	0.0455
R_w[a]	0.0828	0.1383	0.1383	0.0997
GOF	0.979	0.979	1.040	1.017
CCDC Deposition	1023398	1023397	1034753	992606

[a] $R = \Sigma ||F_o| - |F_c|| / \Sigma |F_o|$ and $R_w = (\Sigma \omega(|F_o| - |F_c|)^2 / \Sigma \omega F_o^2)^{1/2}$.

Table 3. Cyclic voltammetric data for **L3-L5** and complexes (mV).

	L3				**L4**				**L5**			
	$E_{½}$	$\triangle E_{½}$	E_p	$\triangle E_p$	$E_{½}$	$\triangle E_{½}$	E_p	$\triangle E_p$	$E_{½}$	$\triangle E_{½}$	E_p	$\triangle E_p$
Free **L**	23(72)		914		177(120)		1022		138(85)		805	
Cu^{2+}	22(81)	-1	931	17	230(117)	53	1070	48	187(86)	49	948	143
Hg^{2+}	84(66)	61	977	63	251(42)	74	1107	85	159(237)	21	1033	228
Zn^{2+}	-	-	-	-	-	-	-	-	153(128)	15	928	123

[a] $E_{½}$ values are the half-wave potentials of the ferrocene unit and are quoted relative to FcH /$[FcH]^+$. The values in mV of $|E_{pa}- E_{pc}|$ are given in brackets.

[b] E_p values are oxidation peak potentials of the anthracene unit and are quoted relative to FcH /$[FcH]^+$.